# Study of couple efficiency in grating couplers

Author: Carles Bennassar i Formentí
*Facultat de Física, Universitat de Barcelona, Diagonal 645, 08028 Barcelona, Spain.*

Advisor: Elena López Aymerich and Albert Romano Rodrıíguez

**Abstract:** In this work we study the light coupling efficiency between a silicon on insulator grating coupler and an optical fiber. We have done electromagnetic simulations by using the finite-difference time-domain method via MEEP Python library. Two different 2D points of view have been carried out to parameterize the grating coupler in the near-infrared region. With the top view, the grating starting parameters, the silicon ridge width, and the grating period, have been determined and the duty cycle is studied. With the side view, the coupling angle and the grating heights have been found.

## I. INTRODUCTION

This work has been done as a contribution for an extensive UB research project directed by Prof. Albert Romano. The project is about evaluating the light transmission through photonic crystals (PC). Biological material will be placed on top of the PC to be studied. Illuminating the system with an optical fiber (OF), will cause the degradation of the biological tissues due to the diameter size of the OF light beam. Therefore, in this work a silicon waveguide structure able to couple the light to illuminate the PC without damaging the biological tissues will be studied.

The usage of Silicon-on-Insulator (SOI) substrate has been considered. Structures fabricated on SOI take advantage of the high refractive index difference between $Si$ and $SiO_2$ to make very thin single mode waveguide structures. There are basically two different approaches for constructing them: edge-coupling and grating-coupling. The first one, places the source in the same plane of the waveguide. It can give rise to low light transmission losses, but requires complicated post-fabrication processes, making it expensive and unable for mass production [1]. The second approach, grating coupling (GC), places the source above it and does not have alignment problems. It is easy and cheap to produce, but give rise to important light losses. To minimise them, a precise configuration is required, both for the light source and for the grating parameters.

In this work a GC on a SOI substrate has been chosen to be studied and parameterized. An OF, as light source, is placed above the GC. It changes the plane of the light transmission, from vertical to horizontal plane, in the waveguide direction. GC couples the light using a serrated saw like converter (Fig.(1)).

Coupling light means making light to propagate from a first medium to a different one. GC does it by adapting progressively the refractive index between the two media (background-silicon). This can be understood with the effective medium theory and the so-called effective refractive index [9]:

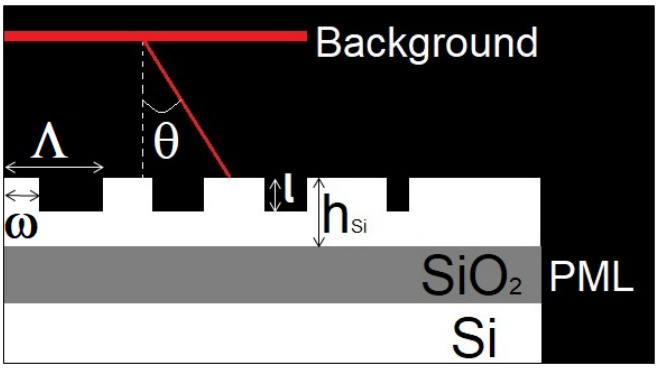


FIG. 1: Sketch of a SOI GC. Parameters $\omega$, $\Lambda$, $\theta$, $l$ and $h_{Si}$ shown.

$$n_{eff}^{TM} = \frac{1}{\sqrt{\frac{d}{n_{Si}^2} + \frac{(1-d)}{n_{bckg}^2}}} \tag{1}$$

Where $n_{eff}$ (1) is the effective refractive index of the GC and depends on: the index of the input light medium (background, $n_{bckg}$), the index of the grating used material ($n_{Si}$) and the duty cycle or fill factor ($d$) (2).

$$d = \omega/\Lambda \tag{2}$$

The duty cycle is defined as the ratio of $\omega$, the silicon ridge width, and $\Lambda$, the grating period. These parameters can be seen in Fig.(1).

The coupling angle $\theta$, calculated by the first order Bragg condition for a GC [8].

$$n_{eff} - n_{bckg} \cdot sin(\theta) = \frac{\lambda_{Src}}{\Lambda} \tag{3}$$

The Bragg condition (3) depends on: $n_{eff}$, $\lambda_{Src}$ and $\Lambda$, see also Fig.(1).

To achieve the best coupling efficiency (CE) all the parameters in equations (1), (2) and (3) must be properly tuned. And, to properly do a waveguide, $d$ has to progressively increase until $d = 1$ to achieve $n_{eff} = n_{Si}$ (1).

These discussions have been carried out by simulations. Using MEEP [4], an open source Python library, a self developed program has been used. The program has been published in my public GitHub `repository` [6]. The project has different files for each function, so it will be easier to make modifications or implement new features.

## II. COMPUTATIONAL METHODS

The Python library MEEP uses one of the many methods available to calculate computational electromagnetism, the Finite-Difference Time-Domain (FDTD) method [2]: it is suitable for dielectric materials and in the Near Infrared (NIR) wavelength range (WLR) [5]. FDTD method solves the derivative form Maxwell curl equations in the time domain. Following a Yee cell procedure, derivatives are replaced by differences and the fields are calculated in separate cells. This allows the location of the field components at offsets using central-difference approximation considering only the nearest cell interaction. Once the fields are properly calculated in each cell, to study the light transmission between the source and the end of the grid, the Poynting vector is used. MEEP can get the power of the electromagnetic flux for a given frequency $\omega$ in a certain plane by:

$$P(\omega) = RE\left[\hat{n} \cdot \int E^*_\omega(x) \times H_\omega(x) d^2x\right] \tag{4}$$

Where $E_\omega(x)$ and $H_\omega(x)$ are the perpendicular single wavelength fields for the $\hat{n}$ direction.

To calculate (4) for a wide WLR, the fields need to be calculated by accumulating their Fourier transforms for every point in the flux plane via summation over the discrete $n$ time steps.

$$\tilde{f}(\omega) = \frac{1}{\sqrt{2\pi}} \sum_n e^{i\omega n \Delta t} f(n\Delta t)\Delta t \approx \frac{1}{\sqrt{2\pi}} \int e^{i\omega t} f(t) dt \tag{5}$$

When introducing a certain angle in the source ($\theta$ in Fig.(1)), $\hat{n}$ and the Poynting vector (4) will not be parallel. Equation (5) will introduce an amplitude term that will result in complex fields:

$$e^{i2\pi K n \Delta t} \tag{6}$$

equation (6) is called power-amplitude (PA), with $K = cos\theta$ [7].

## III. SIMULATIONS

To correctly compute the CE in GC, 3D simulations should be carried out, but they are very resource and time-consuming. To circumvent this issue, two 2D simulations have been proposed: top view and side view (Fig.(2)).

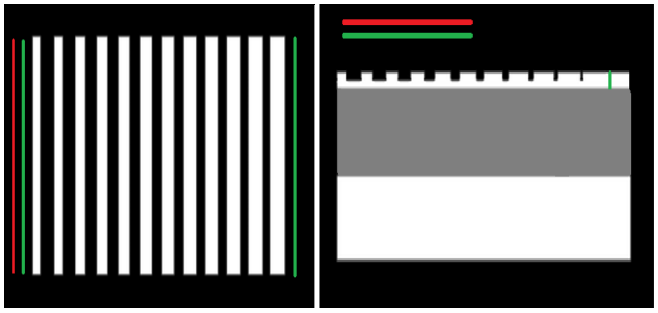

FIG. 2: Schematic representation of the $\varepsilon$ distribution. At left top view, at right side view. Black for water, white for $Si$, grey for $SiO_2$, red for source and green for detectors.

The simulations have been developed using a light ray beam with a Gaussian power amplitude distribution for $\lambda$ within the WLR $\lambda \in [1.35, 1.55\mu m]$. The cell size has been set according to a given number of silicon blocks. 24 blocks has resulted in a good compromise between reasonable computational times (as it increases with the addition of blocks) and enough number of blocks to assume that the coupling light will not change by adding more blocks. Additionally, the cell has $1\mu$m of perfect matching layers (PML) to absorb any incoming electromagnetic wave at all frequencies and angles of incidence at the boundaries of the computational cell [3]. The background has been set to water to simulate our experimental problem, which will be submerged due to the biological application.

In both simulations two flux detectors have been implemented (green lines in Fig.(2)). One of them close to the source, (red lines in Fig.(2)), and with the same size to be able to compute the Poynting vector (power) of the incident ray light. The other, at the end of the grid, with the size and orientation of the last silicon tooth.

To calculate the CE two simulations are run. The first one, with an empty cell (equivalent to a white measure), just with the source and the detectors. This simulation measures the light recorded by the first detector avoiding the reflection effects of the studied structure. The second simulation, is used to calculate the light into the last detector through all the GC.

With both data simulations, CE is calculated as:

$$T(\omega) = \frac{P_{out}(\omega)}{P_{in}(\omega} \tag{7}$$

where $P_{in}$ stands for the flux detected by the first detector in the white simulation, and $P_{out}$ the flux for the second detector in the simulation containing all the structure.

### A. Top view simulations

Top view simulations, have been used to study the $n_{eff}$ (1) accommodation from the source medium to the silicon medium.

Fig.(2), left, shows a scale sketch of a grid example of the cells used in these simulations. This is a simplified 2D simulation which has: two media, water (black) and silicon (white), the source and the two mentioned detectors. The vertical size for the $Si$ blocks has been arbitrarily chosen to avoid large simulation times. The black contours of the image represent both, water and PML.

As known from the Snell's law and Fresnel equations, light will not easily propagate between two media with high $n$ difference. Therefore, the $d$ (2) variation of the GC has been studied to progressively increase $n_{eff}$ to avoid a complete field reflection inside the GC. To do so, $\Lambda$, $\omega$ and the linear apodization factor, the increment of the block width, have been tested.

Firstly, for the $\Lambda$ values $0.9, 1.0$ and $1.1\mu m$, every $\omega \in [0.3, 0.6]$ with a $0.025$ $\mu m$ interval have been simulated. These parameters have been chosen based on the resolution of the manufacturing processes and literature [10]. With this an $n_{eff}$ that does not give rise to a full field reflection at the beginning of the GC, due to the big contrast between $n_{eff}$ and $n_{water}$ has been set.

Once determined the optimal pair of $\Lambda$ and $\omega$, simulations keeping $\Lambda$ constant and linearly increasing $\omega$, for every tooth in the grid, has been carried out. Different increases of $\omega$ can be seen in Fig.(2) left and right. This is a commonly used approach [10] to adapt the $n_{eff}$ of a GC (1).

### B. Side view simulations

The purpose of side view simulations has been to study the light coupling between the source (OF) and the SOI GC.

A scale image for the other 2D simplified simulation can be seen in Fig.(2), right. The initial SOI structure parameters for this simulation have been set according to the paper [11]. In the vertical direction, the first two layers of $Si$ and $SiO_2$ are $2\mu m$ thick. The grating parameters are $h_{Si} = 0.29\mu m$ thick and the etching, $l = 0.07\mu m$, see Fig.(1). In the horizontal direction the best $\Lambda$ and $\omega$ configuration found in the top view simulation has been used for the $Si$ blocks (teeth) width and positions. And the layer's width has been set by: $Width = \Lambda \cdot 24 blocks$ to complete the SOI GC structure.

The starting point has been to find the inclination of the source, $\theta$ value (3) (Fig.(1)), giving us the best CE.

To simulate the correct incidence angle of the light of the source, MEEP introduces the k-point function along with a PA function (6), which instead of tilting the source, tilts the fields in the desired angle, which produces the same effect.

With GC experiments, small angles are used. Usually the best coupling angles are around 8 or 13 degrees [10]. In consequence, we have studied all angles between 2 and 30 degrees in intervals of $0.25°$. This study has been done with one configuration of $\Lambda$ and $\omega$, and without changing the duty cycle $d$ (2). The best incidence angle has been set as the one that gives the optimal CE at the end of the grid.

Once the best coupling angle $\theta$ was found, a study for the best parameters such as $l$, $h_{Si}$ and the source position has been done. Same procedure as in top view simulations has been carried out: starting from $h_{Si} = 0.29\mu m$, $l = 0.07\mu m$ [11] different configurations in $0.01\mu m$ intervals for each parameter has been simulated. Finally, the source position has been tuned.

In this section the increase of the duty cycle effects have not been studied, considering that the best coupling angle $\theta$ shall be the same as by keeping $d$ constant.

## IV. RESULTS

### A. Efective refractive index adaptation

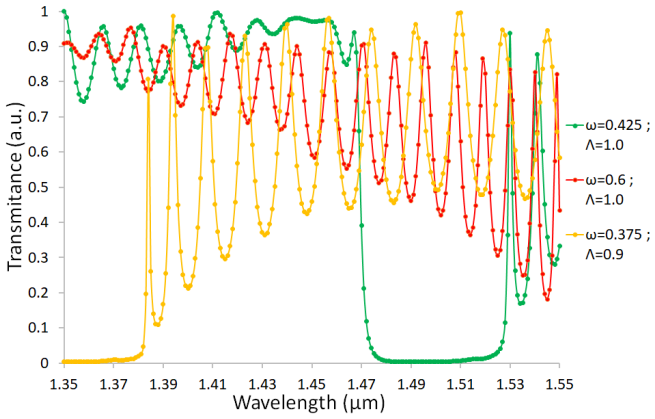


FIG. 3: Couple light transmission over 24 blocks of silicon for different configurations of $\Lambda$ and $\omega$.

In Fig.(3) the transmission calculated as (7), for the light of a Gaussian source emitting light within the WLR $\lambda \in [1.35, 1.55\mu m]$ can be seen. The study for different configurations of $\Lambda$ and $\omega$ resulted in a few null transmittance configurations. The vast majority of configurations resulted in an average transmission of approximately 30-50%, with completely different shapes. A particular case can be seen in yellow line. Some configurations gave higher transmission, around the 90 % in average, as the one with 84.4% of transmission in red line.

Finally, the one with the highest average transmission is shown in green line with a 92.79%. With these parameters, $\Lambda = 1.0\mu m$ and $\omega = 0.425\mu m$ the GC has an $n_{eff} = 1.67$ (1), much closer to the background (water) than to the silicon refractive index. Green line shows an excellent CE within the WLR $\lambda \in [1.35, 1.47\mu m]$. It oscillates at lower $\lambda$ and becomes more constant by increasing it. Green line achieves almost a constant transmission around $\lambda = 1.45\mu m$. There is a band gap with null transmission between 1.47 and 1.53 $\mu m$. Water has an

absorption peak in this range (around $\lambda = 1.5\mu m$), which makes it not useful for our applications. For this reason, all the mentioned average transmission have been calculated within the $\lambda \in [1.35, 1.47\mu m]$ and a source below the water absorption peak WLR should be considered.

With these chosen parameters, the increase of the duty cycle (2) has been studied. In Fig.(4) the comparative between CE for an increment of $\Delta d = 20\%$ for 48 blocks, and for constant $d$ is shown.

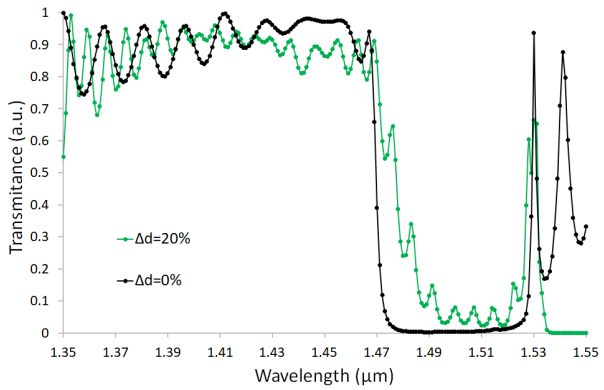


FIG. 4: Light transmission comparison between constant and increasing $d$ for $\Lambda = 1.0\mu m$, $\omega = 0.425\mu m$.

Green line, shows a high performance providing almost the same CE found with constant $\Lambda$ and $\omega$ for just 24 blocks, black line. In comparison, at the beginning, the oscillation of the CE is similar, though it does not become constant around $\lambda = 1.45\mu m$. Also in contrast, the CE of green line decays in transmission % for increasing $\lambda$, until it arrives at the same band gap as in the constant $\omega$ case. This time without such abruptly decay and without giving a 0% of light transmission. For this $d$ increasing rate, the CE, has resulted worse than with the constant $d$ case, but good enough to be considered suitable for the experimental purpose.

The last teeth of the GC for the green line scenario has an $\omega = 0.625\mu m$, this implies an $n_{eff} = 1.947$ (1) for the end of the GC. This value is still far away from the desired $n_{eff} = n_{Si}$. However, when a full $n_{eff}$ coupling ($n_{eff} = n_{Si}$) was attempted in a 48 block cell, a null CE resulted. This happens because in this case the changing rate of the $n_{eff}$ is too large. In a difference of 3 blocks $\Delta n_{eff} = 0.0848$ whereas in the $\Delta d = 20\%$ case for 10 blocks $\Delta n_{eff} = 0.0442$.

### B. Light coupling

The CE for different $\theta$ angles has resulted in the graph in Fig.(5), where several results are shown. In dark blue a narrow but high peak of transmission is shown, reaching almost a 90% average CE for $\lambda \in [1.43, 1.445\mu m]$ with a maximum of 93.5%. Similar results have been obtained for $\theta \in [7.5, 9.75°]$ with almost the same CE, suggesting

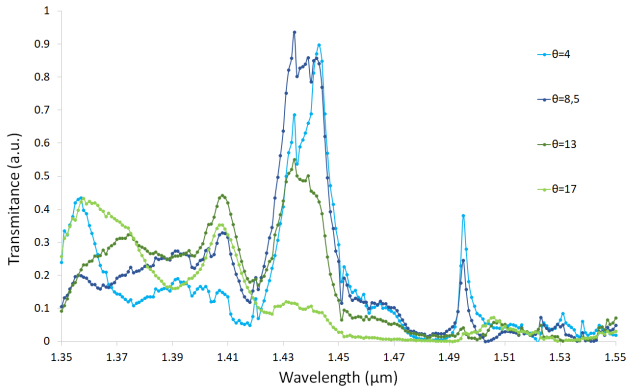


FIG. 5: Plots of the CE for the frontal cut view simulation for different source angle ($\theta$) with $\Lambda = 1.0\mu m$, $\omega = 0.425\mu m$, $h_{Si} = 0.29\mu m$ and $l = 0.07\mu m$ .

that the tilt of the source is not very sensitive to small variations. For lower angles, light blue line, alike transmission in shape but lower in intensity has been obtained, with a central peak narrower than the one seen in dark blue line. While increasing the angle -green lines- the CE was decaying in average and for even greater angles, almost null transmission has been obtained.

The results agree with the expected behavior about GC, which uses low angles for the best CE [11], and differs a bit with the first order Bragg condition (3):

| $\lambda(\mu m)$ | $\theta(°)$ |
|---|---|
| 1.35 | 13.92 |
| 1.45 | 9.52 |
| 1.55 | 5.18 |

TABLE I: Angle calculated with Bragg condition (3), for different $\lambda$.

From the values in Table I it can be seen that for the highest peak, of the blue line in Fig.(5), the angle should be around 9.52° and not 8.5°. As the Bragg condition formula is used for infinite gratings [8], these results have to be taken as a guide.

Fig.(6) shows the comparison for the CE study that has been done by modifying the parameters: $h_{Si}$, $l$ and $h_{Source}$ and the results for the starting parameters. Both with the already discussed parameters: $\theta = 8.5$, $\Lambda = 1.0\mu m$ and $\omega = 0.425\mu m$. The greatest improvement for the CE has been obtained when: $l = 0.06\mu m$, $h_{Si} = 0.3\mu m$ and $h_{Source} = 0.5\mu m$, shown in blue line. As can be seen, the CE shows a high transmission, with an average of 78.8% for a wider WLR than the one observed on the green line. The blue line also has higher peaks than the green one in certain $\lambda$, such as $\lambda = 1.42\mu m$ peak with a transmission of 98.4%.

Improving the CE by tuning the GC was something expected, as $l$ and $h_{Si}$ taken form the documentation [11], were specified for another $\Lambda$ and $\omega$ configuration. Finally, it is important to point out that thanks to these results,

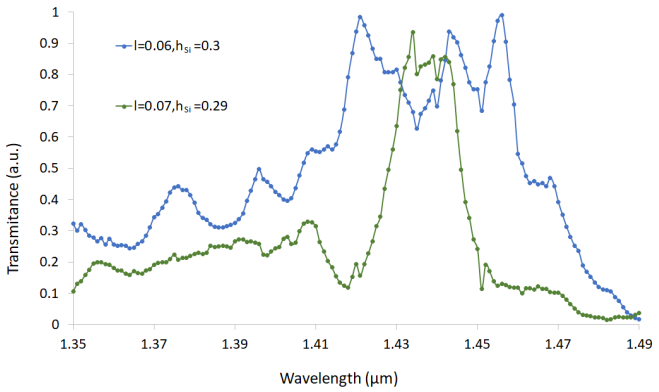


FIG. 6: Comparison of the CE for the frontal cut view simulation with selected parameters [11] (green line) and studied ones (blue line) for $\theta = 8.5°$.

the WLR for the OF that will be used in our experiments, has been narrowed down to $\lambda \in [1.40, 1.47\mu m]$.

## V. CONCLUSIONS

Suitable parameters for the beginning of a waveguide based in a silicon on insulator grating coupler were found via 2D simulations and sectioning the problem in smaller ones.

With the top view, the grating period, the silicon ridge width and the increase of the duty cycle that gave us the highest light coupling efficiency have been determined for a grid with 48 silicon blocks. All these parameters have proved to be highly sensitive to small variations, changing from a high CE to a null transmission by varying one of them just $0.025\mu m$.

In side view, the light coupling was studied. The source tilt, was found to be optimal for low angles, around $\theta = 8.5°$, and the silicon height and etching that gave us the best CE completed all the parametrization for the GC.

Therefore, we can conclude that we have advanced in our research of a GC able to illuminate PC without having to illuminate all the system as with an OF, designing a GC that reaches $n_{eff} = 1.947$ with a high CE.

The $n_{eff}$ still needs to be further studied to try to be adapted until $n_{eff} = n_{Si}$.

### Acknowledgments

I would like to thank my two advisors, Elena for being always accessible with a positive attitude and for making easier all the process for this work. And Albert, providing all his experience to untangle the work when I could not see how. And, as it may be the only opportunity I will have, I have to thank from the heart my parents and brother who have helped me so much in all this process that has been the Physics degree.

[1] Marchetti R, et al. "Coupling strategies for silicon photonics integrated chips" Photonics Res. 2019, 7, 201–239.
[2] Karl S. Kunz and Raymond J. Luebbers. The Finite Difference Time Domain Method for Electromagnetics. 1st. ed. (CRC PRESS, Florida, 1993).
[3] John B. Schneider "Understanding the Finite-Difference Time-Domain Method" (2021)
[4] http://ab-initio.mit.edu/meep (Last visited 11/05/2021).
[5] Oskooi, Ardavan F. et al. "Meep: A flexible free-software package for electromagnetic simulations by the FDTD method." Computer Physics Communications 181.3 (2010): 687-702.
[6] Carles Bennassar GitHub repository `https://github.com/banasa44/TFG_Carles_Bennassar_wvguide_sim`.
[7] `https://github.com/NanoComp/meep/blob/master/doc/docs/Python_Tutorials/Basics.md` (Last visited 15/05/2021).
[8] Yun Wang. "Grating Coupler Design Based on Silicon-On-Insulator" (B.Sc., Shenzhen University, 2011).
[9] T. Kämpfe and O. Parriaux. "Depth-minimized, large period half-wave corrugation for linear to radial and azimuthal polarization transformation by grating-mode phase management" (Université de Lyon, 2011).
[10] Marchetti R. et al. "High-efficiency grating-couplers: demonstration of a new design strategy" SCIENTIFIC REPORTS, 7: 16670 (2017).
[11] Taillaert D. et al. "Grating Couplers for Coupling between Optical Fibers and Nanophotonic Waveguides" Jpn. J. Appl. Phys. 44: 6071 (2006)